Crystalline tetrazepam as a case study on the volume change on melting of molecular organic compounds

Ivo Rietveld, Philippe Négrier, Maria Barrio, Hassan Allouchi, René Ceolin, Josep-Lluís Tamarit

CRYSTALLINE TETRAZEPAM AS A CASE STUDY ON THE VOLUME CHANGE ON MELTING OF MOLECULAR ORGANIC COMPOUNDS

Ivo B. Rietveld[1,2*], Philippe Negrier[3], Maria Barrio[4], Hassan Allouchi[5], René Ceolin[4], Josep-Lluís Tamarit[4*]

[1] SMS Laboratory (EA 3233), Université de Rouen-Normandie, Place Émile Blondel, Mont Saint Aignan 76821, France

[2] Faculté de Pharmacie, Université Paris Descartes, USPC, 4 avenue de l'observatoire, 75006, Paris, France

[3] LOMA, UMR 5798, CNRS, Université de Bordeaux, F-33400 Talence, France

[4] Grup de Caracterització de Materials, Departament de Física and Barcelona Research Center in Multiscale Science and Engineering Universitat Politècnica de Catalunya, EEBE, Campus Diagonal-Besòs, Av. Eduard Maristany 10-14, 08019 Barcelona, Catalonia, Spain.

[5] EA 7502 SIMBA, Synthèse et Isolement de Molécules BioActives, Laboratoire de Chimie Physique, Faculté de Pharmacie, 31, Avenue Monge, 37200 Tours, France

* Corresponding authors : ivo.rietveld@univ-rouen.fr, josep.lluis.tamarit@upc.edu

ABSTRACT

The volume change on melting is a rarely studied quantity and it is not well understood even if it must reflect the changes in interaction between the solid and the liquid state. It is part of the solid-state information for materials and pharmaceuticals and it is important for the reliability of polymorph stability study results. Using the crystal structure of monoclinic tetrazepam at 150 K and at room temperature, in addition to powder X-ray diffraction as a function of the temperature, the specific volume of tetrazepam has been determined over a large temperature domain. In combination with a pressure-temperature curve for the melting of tetrazepam, its volume change on melting could be determined. With this information and previous data from the literature, the assumption that the volume of the solid increases on average with 11% on melting has been investigated. It can be concluded that this value is not constant; however so far, no simple relationship has been found to relate the solid state to its volume change on melting and using 11% remains best practice. A comparison of the tetrazepam crystal structure with diazepam and nordiazepam has been provided too.

Keywords:

Crystal structure; specific volume; calorimetry; phase behavior; phase diagram; X-ray diffraction; molecular interaction

1 INTRODUCTION

Once an active pharmaceutical ingredient (API) has been synthesized, in addition to the toxicological and activity measurements, a preliminary physical characterization is carried out too. The latter is important because once the molecule is considered to be viable API, it will need to be formulated in the most appropriate way. Although the formulation may ideally depend on the activity and patient requirements, unfortunately often the physical behavior has its demands too. The properties of the solid form such as salts, co-crystals, or hydrates and polymorphism may lead to a number of difficult questions to answer or to unexpected problems even if the formulation itself is liquid-based (Bauer et al., 2001; Céolin and Rietveld, 2015; Chaudhuri, 2008; Rietveld and Ceolin, 2015). It is obvious that from an industrial point of view, quick answers with as little as possible experimental effort are preferred, as long as the answers can be trusted. In addition, it may be that certain measurements cannot be carried out due to decomposition or the absence of sufficient API in the early stages of development, when choices nonetheless will have to be made about formulation that could affect 2nd and 3rd phase results due to bioavailability.

It is nowadays customary to carry out experimental and in-silico polymorph screening. However, once the existing polymorphs (i.e. the experimentally verified polymorphs) have been determined, it is not always easy to determine the stability ranking of the polymorphs and the conditions at which the ranking applies. It is for this reason that the method for constructing topological pressure-temperature phase diagrams has been developed (Ledru et al., 2007; Toscani et al., 2002). This method can be used to obtain a full map of the stability ranking between polymorphs over the entire temperature and pressure domain. With such a phase diagram, it will be easy to judge whether an API may be sensitive to compression in tableting for example or on heating during manufacturing or also storage. Such topological phase diagrams, that mainly consist of extrapolations obtained through standard laboratory experiments such as differential scanning calorimetry and X-ray diffraction, can guide decisions whether temperature or pressure should be further explored or that one polymorph can be safely considered the most stable one.

To ensure that the topological phase diagrams are as trustworthy as they can be, it is important that they are based on as many pertinent experimental data as possible. In that way, statistics and the outliers will help discerning the boundaries of applicability of the topological method. Hence, this paper explores the statistics of the volume change on melting of APIs, one of the quantities that is frequently used in the

construction of topological phase diagrams. The volume change between a solid polymorph and the liquid, $\Delta_{fus}v$, at ordinary pressure is necessary to calculate the slope of the melting curve in the pressure-temperature phase diagram. The slope is given by the Clapeyron equation:

$$dP/dT_{fus} = \Delta_{fus}S/\Delta_{fus}v = \Delta_{fus}H/(T_{fus}\,\Delta_{fus}v) \quad (1),$$

where $\Delta_{fus}H$ and $\Delta_{fus}v$ are the enthalpy and volume changes, respectively, on melting at the melting temperature T_{fus}.

However, while the melting temperature and enthalpy change of fusion can be obtained easily by differential scanning calorimetry, the volume change $\Delta_{fus}v$ is by contrast almost never measured. It can be done by measuring the densities of the solid and the liquid as a function of the temperature; however, this is seldom carried out, because thermal degradation occurs frequently (in particular for drug substances), while the sample is kept in the molten state, thus preventing the specific volume of the melt from being correctly determined (Allouchi et al., 2014; Barrio et al., 2012; Brown and Glass, 2003; Henriet et al., 2016; Huang et al., 2017; Mahé et al., 2013; Rietveld et al., 2018; Tetko et al., 2014; Valentini et al., 2018).

When density measurements of the liquid cannot be performed, a possible way to acquire additional data consists of measuring the temperature and enthalpy of fusion of the solid in question in combination with the pressure-temperature melting curve. Using the Clapeyron equation (eq. 1) the volume change on melting at the melting temperature and at normal pressure can then be obtained. After adding this value to the specific volume of the solid at T_{fus} and at normal pressure, which can be obtained from the thermal expansion of the solid, the specific volume of the liquid at T_{fus} is obtained. This allows the calculation of the ratio v_{liquid}/v_{solid} at T_{fus} and at normal pressure.

Previous determinations indicate that the volume change on melting for most APIs and other small organic molecules is such that the ratio v_{liquid}/v_{solid} is about 1.10-1 .12, *i.e.* a value that can tentatively be considered to be almost constant irrespective of the organic molecular solid (Barrio et al., 2017; Céolin and Rietveld, 2015; Goodman et al., 2004). Nevertheless, this experimental observation needs more support by a larger number of experimental values. The question of whether the ratio is constant remains therefore open, as will be discussed in this paper together with the predictive character of the abovementioned ratio.

In the present paper, the solid state of monoclinic tetrazepam (inset in Figure 1), an active pharmaceutical ingredient with muscle relaxant properties is presented. A comparison of its crystal structure with that of the similar molecules, diazepam and nordiazepam, is provided. Finally, making use of the specific volume obtained as a function of the temperature by powder diffraction, the volume difference between the solid and liquid on melting has been determined and the statistics on this quantity have been discussed.

2 EXPERIMENTAL

2.1 SAMPLES

Single crystals of tetrazepam, whose crystal structure was solved previously at 293 K (Allouchi et al., 2019), were obtained by slowly evaporating solutions in methanol at room temperature using a powder of medicinal grade kindly supplied by Daiichi Sankyo France SAS. Since the X-ray diffraction profile of the commercial sample was the same as the calculated one from the crystal structure, the powder was used as such, and the crystal structure was redetermined at 150 K.

2.2 SINGLE CRYSTAL X-RAY DIFFRACTION

X-ray diffraction intensities were collected at 150 K on an Xcalibur-2 diffractometer with Sapphir-2 CCD area detector and monochromatized Mo-Kα radiation (0.71073 Å). The collection method involved ω-scans having a width of 1°. The data collection, unit-cell refinement, and data reduction were performed using the CrysAlis Pro, Oxford Diffraction Ltd. software package (Agilent-Technologies, 2014). Analytical numeric absorption correction was carried out using a multifaceted crystal model(Clark and Reid, 1995). The positions of non-H atoms were determined and refined by the SHELXS program (Sheldrick, 2008). Non-hydrogen atoms were first refined isotropically followed by anisotropic refinement by full matrix least-squares calculations based on F^2 using SHELXe (Hubschle et al., 2011). The positions of the H-atoms were deduced from coordinates of the non-H atoms and Fourier synthesis. H-atoms were included for structure factor calculations but not refined. Publication materials were generated using WinGX (Farrugia, 2012) and Mercury-3.3 (Macrae et al., 2008).

2.3 HIGH-RESOLUTION X-RAY POWDER DIFFRACTION (HR-XRPD)

XRPD measurements were performed with a vertically mounted INEL cylindrical position-sensitive detector (CPS-120) using the Debye–Scherrer geometry and transmission mode. Monochromatic Cu-Kα_1 (λ = 1.54056 Å) radiation was selected by means of an asymmetrically focusing incident-beam curved quartz monochromator. Measurements as a function of temperature were performed using a liquid nitrogen 700 series Cryostream Cooler from Oxford Cryosystems. Cubic phase $Na_2Ca_3Al_2F_4$ was used for external calibration. PEAKOC application from DIFFRACTINEL software was used for the calibration as well as for the peak position determinations after pseudo-Voigt fittings and lattice parameters were refined by way of the least-squares option of the FullProf suite (Rodriguez-Carvajal, 1993; Rodriguez-Carvajal et al., 2005).

Specimens were introduced in a Lindemann capillary (0.5-mm diameter) and allowed to rotate perpendicularly to the X-ray beam during the experiments to improve the averaging of the crystallite orientations. Before each isothermal data acquisition, the specimen was allowed to equilibrate for about 10 min, and each acquisition time was at least 1 h. The heating rate in between data collection was 1.33 K min^{-1}. The diffraction patterns of tetrazepam, diazepam, and nordiazepam have been recorded as a function of the temperature from about 100 K up to their respective melting points.

2.4 DIFFERENTIAL SCANNING CALORIMETRY (DSC)

Temperature (onset) and heat of fusion were obtained with a Q100 thermal analyzer from TA Instruments at heating rates from 2 to 10 K min^{-1}. The analyzer was calibrated by using the melting point of indium (T_{fus} = 429.75 K and $\Delta_{fus}H$ = 3.267 kJ mol^{-1}). The specimens were weighed using a microbalance sensitive to 0.01 mg and sealed in aluminum pans.

2.5 HIGH-PRESSURE DIFFERENTIAL THERMAL ANALYSIS (HP-DTA)

HP-DTA measurements have been carried out at 2 K min^{-1} using a home-made high-pressure differential thermal analyzer similar to Würflinger's apparatus and operating in the 298 – 473 K and 0 – 250 MPa ranges (Würflinger, 1975). To determine the melting temperature as a function of pressure and to ascertain that in-pan volumes were free from residual air, specimens were mixed with an inert perfluorinated liquid (Galden®, from Bioblock Scientifics, Illkirch, France) as a pressure-transmitting

medium, and the mixtures were sealed into cylindrical tin pans. To check that the perfluorinated liquid was chemically inactive and should thus have no influence on the melting temperature of tetrazepam, preliminary DSC measurements were carried out with a Galden®-tetrazepam mixture on a Q100 analyzer of TA instruments without applied pressure.

3 RESULTS

3.1 THE CRYSTAL STRUCTURE AT 150 K

The crystal structure at 150 K was found to be the same monoclinic $P2_1/c$ structure (Z = 4) as the one solved at 293 K (Allouchi et al., 2019). Structural information can be found in the Supplementary Materials: Crystal and structure refinement data (Table S1), atom labels (Figure S2), fractional coordinates, bond lengths, bond angles, anisotropic displacement parameters, torsion angles and hydrogen bonds (Tables S2 to S6, respectively). The Cambridge Crystallographic Data Centre (CCDC) deposit number 2025809 contains the supplementary crystallographic data for this paper. It can be obtained free of charge from the CCDC via www.ccdc.cam.ac.uk/data_request/cif.

Lattice parameters at 150 K were found to be: a = 12.5260(2) Å, b = 11.2860(2) Å, c = 10.2714(2) Å, β = 102.378(2)°, V_{cell} = 1418.30(4) Å^3, leading to a density (Z = 4) of 1.35232(6) g cm^{-3} and a specific volume of v = 0.73947(4) cm^3 g^{-1}.

3.2 THE SPECIFIC VOLUME OF TETRAZEPAM AS A FUNCTION OF THE TEMPERATURE

Lattice parameters as a function of the temperature have been determined by X-ray powder diffraction measurements between about 150 K and the melting point for tetrazepam, diazepam, and nordiazepam. The corresponding specific volumes of tetrazepam as a function of the temperature are presented in Figure 1. Values of lattice parameters and specific volumes have been compiled in Table S7. Thermal expansion data for diazepam and nordiazepam can be found in Tables S8 and S9.

The values of the specific volume have been fitted to the linear equation:

$$v/\mathrm{cm^3\,g^{-1}} = 0.7169(10) + 1.46(3)\cdot 10^{-4}\, T/\mathrm{K} \qquad (R^2 = 0.996) \qquad (2)$$

The specific volumes from the single crystal data at 293 K (Allouchi et al., 2019) and at 150 K are in close agreement with those obtained by X-ray powder diffraction (Figure 1).

3.3 CALORIMETRIC BEHAVIOR

Calorimetric measurements under normal pressure have been carried out for several samples using heating rates ranging from 2 to 10 K min^{-1}. The results have been compiled in Table S10 in the Supplementary Materials. On heating from room temperature (curve 1 in Figure 2), a single endothermic peak ascribed to the melting of tetrazepam was measured with an onset at T_{fus} = 415.6(1.2) K and an enthalpy change of 88.6(4.6) J g^{-1} (25.6(1.3) kJ mol^{-1}). Upon cooling the melt down to 200 K, no recrystallization-related thermal event was observed.

On reheating, after cooling the melt down to 200 K, a glass transition (midpoint at 315.0(1.0) K) was observed (curve 2 and inset in Figure 2) followed by the recrystallization of the metastable melt and, finally, by the melting of the monoclinic form. It is worth mentioning that the melting process corresponding to samples previously melted takes place at a slightly lower temperature and, for heating rates higher than 5 K·min^{-1} with a smaller enthalpy change. The first experimental fact is associated with a possible decomposition in the liquid state, while the second fact is due to a partial recrystallization because the exothermic process involves also a smaller enthalpy change.

3.4 THERMAL BEHAVIOR UNDER PRESSURE

The temperature of fusion (onset) has been determined at various pressures ranging from 0 to 200 MPa (see Figure 3b) and the pressure-temperature phase diagram has been constructed and is provided in Figure 3a. The values have been compiled in Table S11 of the Supplementary Materials. A slight curvature visible in the experimental solid-liquid equilibrium curve (dashed line as a guide for the eye in Figure 3a) indicates that the pressure dependence of the melting temperature is slightly non-linear, which is caused by the difference in the response to the pressure by the solid and the liquid.

Despite the slight curvature, the data can be fitted with a linear function with reasonable accuracy due to the narrow pressure range:

$$T_{fus}\,(P)/\mathrm{K} = 0.326(11)\,P/\mathrm{MPa} + 415.5(1.0) \qquad (R^2 = 0.99) \qquad (3)$$

4 DISCUSSION

4.1 COMPARISON OF THE STRUCTURE AND ITS THERMAL EXPANSION

The monoclinic structure, $P2_1/c$, of tetrazepam is characterized by dimers through C-H···O (2.72 Å) hydrogen bonds (see Figure 4 left-hand side). Similar dimers are present in related benzodiazepines such as oxazepam, lorazepam, nitrozepam, and clonazepam (Neville et al., 1991, 1992). The stacking of the dimers implies soft van der Waals interactions between them along the *a* axis (see Figure 4). Strong intermolecular hydrogen bonds C-H···O (2.46 and 2.54 Å) as well as C-H···N (2.64 Å) are mainly present along the *bc* plane (see Figure 4 left-hand side). The right-hand side of Figure 4 depicts the Hirshfeld surface of the tetrazepam molecule in its crystal structure with the neighboring molecules and the intermolecular interactions. Characteristic values of hydrogen bonds for tetrazepam at 150 K are given in Table S6 of the Supplementary Materials. For comparison, the packing and the Hirshfeld surfaces of diazepam and nordiazepam are provided in Figure S2 in the Supplementary Materials generated from the structures reported in the literature at room temperature (Camerman and Camerman, 1972; D. Prasanna and N. Guru Row, 2000; Dayananda et al., 2013). Table 1 compares the characteristic hydrogen bond (inter and intramolecular) distances for tetrazepam as well as for diazepam and nordiazepam at room temperature. From Table 1, it can be observed that tetrazepam is the only compound with intramolecular C-H···O hydrogen bonds, while comparable C-H···N bonds, with quite similar characteristic distances are present for all three compounds.

Figure 5 contains the 2D fingerprint plots of the O···H and N···H hydrogen bonds for tetrazepam, diazepam, and nordiazepam. The intermolecular hydrogen bonds are quite similar and show up as spikes (for short d_i and d_e distances) related to the donor atom (upper spike) and to the acceptor atom (lower spike). As for tetrazepam, both short d_i and d_e distances are longer for the O···H bonds than for the other two compounds. On the other hand, the N···H bonds of tetrazepam are shorter and the spikes in the fingerprint plot are more localized, indicating strong interactions; these bonds are weaker for nordiazepam and diazepam (see also Figure S2, Supplementary Materials). It is worth mentioning that for

nordiazepam, the shortest hydrogen bond is the N1-H11···O1 with a distance of only 2.03 Å as the fingerprint plot in Figure 5 top-right panel demonstrates; this is unmatched in the other compounds.

Table 1. Characteristic intra- and intermolecular hydrogen bond distances in tetrazepam and related compounds diazepam and nordiazepam at room temperature

Hydrogen Bonds	**Intermolecular**		**Intramolecular**	
Compound	D-H···A	d(H··A) /Å	D-H···A	d(H··A) /Å
Tetrazepam	C2-H2B···O1	2.51	C16-H16A....N2	2.52
	C7-H7···O1	2.61	C16-H16A....O1	2.47
	C10-H10A···O1	2.75		
	C9-H8···N2	2.70		
Diazepam	C24-H24···O1	2.44		
	C22-H22···O1	2.53	C26-H26···N2	2.48
	C13-H13···N2	2.81		
	C15-H15···N2	2.79		
Nordiazepam	C15-H3···O1	2.65	C12-H2···N2	2.51
	N1-H11···O1	2.03		
	C3-H8···N1	2.79		
	C6-H10···N2	2.79		

The contributions of the relevant intermolecular contacts to the Hirshfeld surface areas are reported in Figure 6 for tetrazepam and the related molecules diazepam and nordiazepam. It can be seen that the relative contribution concerning the hydrogen bond O···H is smaller for the tetrazepam and higher for nordiazepam, as the spikes of Figure 5 reveal. On the other hand, the contribution of the N···H is larger for tetrazepam. The whole of the O···H, N···H and Cl···H contributions account for the 29.4, 26.6 and 28.4% for tetrazepam, diazepam and nordiazepam, respectively, of the total surface contacts demonstrating the relevance of the hydrogen bonds in all these structures.

In order to get an idea of the strength and the anisotropy of the intermolecular interactions of the monoclinic phase of tetrazepam, the isobaric thermal expansion tensor (Salud et al., 1998) has been determined. The deformation dU of a crystal due to a change of temperature dT is minimal in the directions of the strongest intermolecular interactions and vice versa. Thus, the eigenvalues and eigenvectors of the second-rank isobaric thermal expansion tensor α_{ij}, with $dU = \alpha_{ij} dT$, give insight into the strength of the intermolecular interactions along three perpendicular directions in the crystal, commonly referred to as "hard" and "soft" directions for strong and weak interactions respectively (Salud et al., 1998).

The lattice parameters of tetrazepam were fitted as a function of the temperature using a standard least-squares method for each parameter. Table S7 (Supplementary Materials) contains the refined lattice parameters as well as the coefficients of the polynomial equations together with the reliability factor, defined as $R = \sum \frac{(l_o - l_c)^2}{l_c^2}$, where l_o and l_c are the observed and calculated lattice parameters, respectively. The program DEFORM (Filhol et al., 1987) was used for the calculation of the tensor. The same procedure was followed for diazepam and nordiazepam. Powder X-ray diffraction patterns have been acquired as a function of the temperature and the lattice parameters have been fitted using the published monoclinic ($P2_1/c$) structures of diazepam (Dayananda et al., 2013) and nordiazepam (D. Prasanna and N. Guru Row, 2000).

For a monoclinic lattice, the tensor is completely defined by the principal coefficients, α_1, α_2, and α_3, an angle between the direction of one of the principal directions ($\boldsymbol{\alpha_3}$, in the present case) and the crystallographic axis $\boldsymbol{a}$, the $\boldsymbol{\alpha_2}$ eigenvector being parallel to the 2-fold axis $\boldsymbol{b}$ of the monoclinic crystal. The data can be found in Tables S8 and S9 in the Supplementary Materials.

Figure 7 represents the eigenvalues as a function of the temperature for the three compounds. In the case of tetrazepam, the strongest intermolecular interactions reflected by negative tensor values indicating contraction on heating ($\boldsymbol{\alpha_3}$ direction) can be found parallel to the *bc* plane and close to the ***c*** crystallographic direction, while the soft direction ($\boldsymbol{\alpha_1}$) is rather close to the ***a*** direction, in perfect agreement with the planes in which strong intermolecular hydrogen bonds appear. In diazepam, the soft direction appears close to the two-fold axis ***b***, while the strongest interactions are within the *ac* plane and the hardest direction ($\boldsymbol{\alpha_3}$ eigenvector) is close to the crystallographic ***a*** direction related to strong hydrogen bonds (see Figure S2 of the Supplementary Materials). In diazepam and nordiazepam, hard directions result in only slightly negative eigenvalues (contraction) unlike tetrazepam for which contraction exists in one direction along the whole temperature range from 100 K to the melting temperature. Moreover, whereas tetrazepam and diazepam are entirely anisotropic in their thermal expansion, the depiction of the thermal expansion tensor of nordiazepam resembles that of a donut, with a slight contraction along the **c** direction and a virtually isotropic expansion in the two other directions.

4.2 STATISTICAL ANALYSIS OF THE SPECIFIC VOLUME OF TETRAZEPAM

The specific volume of tetrazepam as a function of the temperature is represented by eq. 2 and combines data of both X-ray powder diffraction and single crystal X-ray diffraction at 150 and 293 K. The datapoints are presented in Figure 1. Eq. 2 leads to the expansivity for tetrazepam of $\alpha_v = 2.03 \cdot 10^{-4}$ K^{-1}, i.e. close to the mean value of $2.21 \cdot 10^{-4}$ K^{-1} found for solids consisting of small organic molecules (Ceolin and Rietveld, 2017; Céolin and Rietveld, 2015; Rietveld and Céolin, 2015). Nevertheless, the lattice expansion is highly anisotropic; the aspherism index (Weigel et al., 1978) ranges between 0.52 at 150 K and 0.39 at 400 K. The anisotropy is similar to those of tienoxolol (Nicolaï et al., 2013) and ascorbic acid (Nicolai et al., 2017).

With eq. 2, the specific volume of crystalline tetrazepam at its temperature of fusion (i.e. its triple point of 415.6 K) is found to be 0.7774 cm^3 g^{-1}, which becomes 0.777(2) cm^3 g^{-1} with the error taken into account. From eq. 3, the slope of the solid-liquid equilibrium is found to be $dT/dP = 0.326(11)$ K MPa^{-1}. Using the enthalpy of fusion, $\Delta_{fus}H = 88.6(4.6)$ J g^{-1}, and the melting point, $T_{fus} = 415.6(1.2)$ K, and inserting these into the Clapeyron equation (eq. 1) one can calculate the volume change that accompanies the melting transition $\Delta_{fus}v = v_L - v_S = 0.069$ cm^3 g^{-1}. Adding this value to the specific volume of the crystalline solid at

T_{fus} leads to the specific volume of the melt at this temperature. It results in $v_{L,fus}$ (T = 415.6 K) = 0.847(5) $cm^3\ g^{-1}$ and the ratio v_L/v_S at T_{fus} equals therefore 1.089(6), i.e. close to the value of 1.11 ±0.04, previously found for a number of molecular compounds (Barrio et al., 2019; Ceolin and Rietveld, 2017; Céolin and Rietveld, 2015; Céolin and Rietveld, 2020; Rietveld and Céolin, 2015).

Table 2. Ratio between the specific volumes of the liquid (v_L) and the solid (v_S) at the triple point (≈ T_{fus}) and the volume change at the triple point ($\Delta v = v_L - v_S$). I or II following the compound name indicates the polymorph, *X*' being the metastable polymorph at normal pressure.

	compound	T_{fus}/K	$v_L(T_{fus})$ / $cm^3 \cdot g^{-1}$	$v_S(T_{fus})$ / $cm^3 \cdot g^{-1}$	v_L/v_S	$v_L - v_S$ / $cm^3 \cdot g^{-1}$	Reference
1	Paracetamol-I	442.3	0.9091	0.7935	1.14_5	0.1155	Espeau2005
1'	Paracetamol-II	430.2	0.9025	0.7679	1.17_5	0.1346	Espeau2005
2	Prilocaine	311.5	1.000	0.8840	1.13	0.1160	Rietveld2013
3	Rimonabant-I	428.3	0.8284	0.7554	1.11	0.0721	Perrin2013
3'	Rimonabant-II	429.2	0.8289	0.7480	1.11	0.080	Perrin2013
4	Biclotymol-I	400.5	0.9032	0.8000	1.13	0.1032	Ceolin2008
4'	Biclotymol-II	373.8	0.8813	0.8437	1.05	0.0394	Ceolin2008
5	Ternidazole	333.0	0.7989	0.6970	1.15	0.1019	Mahe2011
6	Morniflumate	348.1	0.8062	0.7192	1.12	0.0869	Barrio2017
7	Etifoxine	362.4	0.8599	0.78905	1.09	0.0709	Barrio2019
8	Progesterone-I	402.2	0.9590	0.8801	1.09	0.0789	Barrio2009
8'	Progesterone-II	394.5	0.9521	0.8788	1.08	0.0733	Barrio2009
9	Lidocaine	340.9	1.0337	0.9761	1.06	0.0576	Céolin2010

10	Tetrazepam	415.6	0.8469	0.7774	1.09	0.069	This work

In 2004, Goodman et al. reported on the relationship between organic solid density ρ_S and liquid density ρ_L at the melting triple point T_t (Goodman et al., 2004). In the article, the authors wrote that a "*a simple ratio of the two densities* $\rho_S(T_t)/\rho_L(T_t) = 1.17$ [T_t being the triple point temperature] *was* [previously] *found to be adequate and reliable for most organic compounds*". They proposed to extend this ratio "*to include a temperature dependence for solid density from* T_t *to substantially lower temperatures*" and they concluded that "*the new correlation gives a ratio of solid to liquid density at the triple point of 1.12 instead of 1.17... with an estimated average uncertainty of about 6%*" (i.e., 1,12(7)).

That the ratio of the two densities, i.e. the ratio of the two specific volumes, is constant is an implicit 'working' assumption in Goodman's paper, which should be questioned. The experimental values of v_L/v_S at the melting triple point for a number of organic molecular compounds are compiled in Table 2. These values have also been represented in Figure 8, together with the corresponding error bars. They have been plotted against Δv to facilitate visualization of the variation in the ratios, because the key factors affecting the v_L/v_S ratio are for now unknown.

5 CONCLUSIONS

The structure of tetrazepam has been determined at 150 K as monoclinic with space group $P2_1/c$, the same as previously found at room temperature. The intermolecular interactions concern both intra and intermolecular hydrogen bonds. Soft van der Waals interactions enable stacking of dimers along the ***a*** crystallographic direction, whereas strong intermolecular hydrogen bonds are mainly located along the *bc* monoclinic plane. The hydrogen bond network as well as the intermolecular contacts have been compared through the Hirschfeld surface areas and fingerprint plots to those of the closely related molecules diazepam and nordiazepam.

The analysis reveals that, whereas N···H intramolecular hydrogen bonds are present in all the studied materials, intramolecular O···H hydrogen bonds only appear in the case of tetrazepam. As for the close contacts, studied through the Hirshfeld surface analysis, the O···H, N···H, and Cl···H contributions with respect the total surface contacts are quite similar for tetrazepam, diazepam and nordiazepam (29.4, 26.6 and 28.4% respectively).

Eigenvalues and the associated hard and soft directions of the thermal expansion tensor have been determined for tetrazepam, diazepam and nordiazepam. They demonstrate noticeable differences especially for the direction and intensity in which the respective lattices contract. Tetrazepam in particular exhibits a contraction with increasing temperature over the entire monitored temperature range approximately along the ***c*** crystallographic axis with a thermal expansion tensor value of about 10^{-3} K^{-1}.

Finally, with the analysis of several active pharmaceutical ingredients, it has been demonstrated that the ratio between the liquid and solid specific volumes at the melting point vary within a relatively limited range. Although a greater number of pharmaceuticals must be studied, the trend clearly shows that this ratio is not constant. This is important, because predicting the density of the liquid for pharmaceuticals that can easily decompose in the liquid state (as many APIs do), will allow the calculation of the slope of the solid-liquid equilibrium. This slope in turn will allow the construction of the so-called topological pressure-temperature phase diagram with standard laboratory DSC and XRD data. Finally, the phase diagram specifies the equilibrium conditions of the different polymorphs, which is important for the formulation stage in drug development.

ACKNOWLEDGEMENTS

The authors are grateful for the financial support received within Projects No. FIS2017-82625-P from MINECO and Project No. 2017SGR-042 from the Generalitat de Catalunya.

REFERENCES

Agilent-Technologies, 2014. CrysAlisPro, Version 1.171.37.35 (release 13-08-2014 CrysAlis171.NET) ed.

Allouchi, H., Ceolin, R., Gueiffier, A., Rietveld, I.B., 2019. A network of weak hydrogen bonds in the crystal structure of Tetrazepam. Ann Pharm Fr 77, 121-125.

Allouchi, H., Nicolai, B., Barrio, M., Ceolin, R., Mahe, N., Tamarit, J.-L., Do, B., Rietveld, I.B., 2014. On the Polymorphism of L-Citrulline: Crystal Structure and Characterization of the Orthorhombic delta Form. Cryst. Growth Des. 14, 1279-1286.

340 Barrio, M., Allouchi, H., Tamarit, J.L., Ceolin, R., Berthon-Cedille, L., Rietveld, I.B., 2019. Experimental and
341 topological determination of the pressure-temperature phase diagram of racemic etifoxine, a
342 pharmaceutical ingredient with anxiolytic properties. Int. J. Pharm. 572, 118812.
343 Barrio, M., Maccaroni, E., Rietveld, I.B., Malpezzi, L., Masciocchi, N., Ceolin, R., Tamarit, J.L., 2012. Pressure-
344 temperature state diagram for the phase relationships between benfluorex hydrochloride forms I and II: a
345 case of enantiotropic behavior. J. Pharm. Sci. 101, 1073-1078.
346 Barrio, M., Tamarit, J.L., Ceolin, R., Robert, B., Guechot, C., Teulon, J.M., Rietveld, I.B., 2017. Experimental
347 and topological determination of the pressure temperature phase diagram of morniflumate, a
348 pharmaceutical ingredient with anti-inflammatory properties. J. Chem. Thermodyn. 112, 308-313.
349 Bauer, J., Spanton, S., Henry, R., Quick, J., Dziki, W., Porter, W., Morris, J., 2001. Ritonavir: An extraordinary
350 example of conformational polymorphism. Pharm. Res. 18, 859-866.
351 Brown, M.E., Glass, B.D., 2003. Decomposition of solids accompanied by melting - Bawn kinetics. Int. J.
352 Pharm. 254, 255-261.
353 Camerman, A., Camerman, N., 1972. Stereochemical basis of anticonvulsant drug action. II. Molecular
354 structure of diazepam. J. Am. Chem. Soc. 94, 268-272.
355 Ceolin, R., Rietveld, I.B., 2017. The topological phase diagram of cimetidine: A case of overall monotropy.
356 Ann. Pharm. Fr. 75, 89-94.
357 Céolin, R., Rietveld, I.B., 2015. The topological pressure-temperature phase diagram of ritonavir, an
358 extraordinary case of crystalline dimorphism. Ann. Pharm. Fr. 73, 22-30.
359 Céolin, R., Rietveld, I.B., 2020. Topological pressure-temperature state diagram of the crystalline
360 dimorphism of 2,4,6-trinitrotoluene. Fluid Phase Equilib. 506, 112395-112400.
361 Chaudhuri, K.R., 2008. Crystallisation within transdermal rotigotine patch: is there cause for concern?
362 Expert Opin Drug Del 5, 1169-1171.
363 Clark, R.C., Reid, J.S., 1995. Empirical absorption correction using spherical harmonics, implemented in
364 SCALE3 ABSPACK scaling algorithm. Acta Crystallogr. A51, 887-897.
365 D. Prasanna, M., N. Guru Row, T., 2000. Analysis of weak interactions involving fluorine: a comparative
366 study of crystal packing of some benzodiazepinone drug intermediates and their non-fluorinated
367 analogues. CrystEngComm 2, 134-140.

Dayananda, A.S., Yathirajan, H.S., Gerber, T., Hosten, E., Betz, R., 2013. Redetermination of the structure of 7-chloro-1,3-dihydro-1-methyl-5- phenyl-1,4-benzodiazepin-2(3H)-one, C16H13ClN2O. Zeitschrift für Kristallographie - New Crystal Structures 228, 223.

Farrugia, L.J., 2012. WinGX and ORTEP for Windows: an update. J. Appl. Crystallogr. 45, 849-854.

Filhol, A., Lajzerowicz, J., Thomas, M., 1987. DEFORM.

Goodman, B.T., Wilding, W.V., Oscarson, J.L., Rowley, R.L., 2004. A note on the relationship between organic solid density and liquid density at the triple point. J. Chem. Eng. Data 49, 1512-1514.

Henriet, T., Gana, I., Ghaddar, C., Barrio, M., Cartigny, Y., Yagoubi, N., Do, B., Tamarit, J.-L., Rietveld, I.B., 2016. Solid state stability and solubility of triethylenetetramine dihydrochloride. Int. J. Pharm. 511, 312-321.

Huang, S., O'Donnell, Delpon de Vaux, S.M., O'Brien, J., Stutzman, J., Williams III, R.O., 2017. Processing thermally labile drugs by hot-melt extrusion: The lesson with gliclazide. Eur. J. Pharm. Biopharm. 119, 56-67.

Hubschle, C.B., Sheldrick, G.M., Dittrich, B., 2011. ShelXle: a Qt graphical user interface for SHELXL. J. Appl. Crystallogr. 44, 1281-1284.

Ledru, J., Imrie, C.T., Pulham, C.R., Céolin, R., Hutchinson, J.M., 2007. High pressure differential scanning Calorimetry investigations on the pressure dependence of the melting of paracetamol polymorphs I and II. J. Pharm. Sci. 96, 2784-2794.

Macrae, C.F., Bruno, I.J., Chisholm, J.A., Edgington, P.R., McCabe, P., Pidcock, E., Rodriguez-Monge, L., Taylor, R., Van De Streek, J., Wood, P.A., 2008. Mercury CSD 2.0– new features for the visualization and investigation of crystal structures. J. Appl. Crystallogr. 41, 466-470.

Mahé, N., Nicolaï, B., Allouchi, H., Barrio, M., Do, B., Céolin, R., Tamarit, J.-L., Rietveld, I.B., 2013. Crystal Structure and Solid-State Properties of 3,4-Diaminopyridine Dihydrogen Phosphate and Their Comparison with Other Diaminopyridine Salts. Cryst. Growth Des. 13, 708-715.

Neville, G.A., Beckstead, H.D., Shurvell, H.F., 1991. Fourier transform Raman and infrared study of nitrazepam, nimetazepam, clonazepam and flunitrazepam. Vib. Spectrosc 1, 287-297.

Neville, G.A., Beckstead, H.D., Shurvell, H.F., 1992. An FT-Raman and IR study of oxaxepam, temazepam, lorazepam, and Lormetazepam, Spectroscopicum Internationale. Colloquium (27 ; Bergen 1991-06-09). Polyscience, Morin Heights, PQ, pp. 18-29.

Nicolai, B., Barrio, M., Tamarit, J.L., Ceolin, R., Rietveld, I.B., 2017. Thermal expansion of L-ascorbic acid. Eur. Phys. J. - S.T. 226, 905-912.

Nicolaï, B., Rietveld, I.B., Barrio, M., Mahé, N., Tamarit, J.-L., Céolin, R., Guéchot, C., Teulon, J.-M., 2013. Uniaxial negative thermal expansion in crystals of tienoxolol. Struct. Chem. 24, 279-283.

Rietveld, I.B., Barrio, M., Lloveras, P., Ceolin, R., Tamarit, J.L., 2018. Polymorphism of spironolactone: An unprecedented case of monotropy turning to enantiotropy with a huge difference in the melting temperatures. Int. J. Pharm. 552, 193-205.

Rietveld, I.B., Ceolin, R., 2015. Rotigotine: Unexpected Polymorphism with Predictable Overall Monotropic Behavior. J. Pharm. Sci. 104, 4117-4122.

Rietveld, I.B., Céolin, R., 2015. Phenomenology of crystalline polymorphism: overal monotropic behavior of the cardiotonic agent FK664 forms A and B. J. Therm. Anal. Calorim. 120, 1079-1087.

Rodriguez-Carvajal, J., 1993. Recent advances in magnetic structure determination by neutron powder diffraction. Physica B 192, 55-69.

Rodriguez-Carvajal, J., Roisnel, T., Gonzales-Platas, J., 2005. Full-Prof suite version 2005, Laboratoire Léon Brillouin, CEA-CNRS, CEN Saclay, France.

Salud, J., Barrio, M., Lopez, D.O., Tamarit, J.L., Alcobe, X., 1998. Anisotropy of intermolecular interactions from the study of the thermal-expansion tensor. J. Appl. Crystallogr. 31, 748-757.

Sheldrick, G.M., 2008. A short history of SHELX. Acta Crystallogr. A 64, 112-122.

Tetko, I.V., Sushko, Y., Novotarskyi, S., Patiny, L., Kondratov, I., Petrenko, A.E., Charochkina, L., Asiri, A.M., 2014. How accurately can we predict the melting points of drug-like compounds. J. Chem. Inf. Model. 54, 3320-3329.

Toscani, S., de Oliveira, P., Céolin, R., 2002. Phenomenology of polymorphism IV. The trimorphism of ferrocene and the overall metastability of its triclinic phase. J. Solid State Chem. 164, 131-137.

Valentini, S., Romanini, M., Franco, L., Puiggali, J., Tamarit, J.L., Macovez, R., 2018. Tuning the kinetic stability of the amorphous phase of the chloramphenicol antibiotic. Mol. Pharmaceut. 15, 5615-5624.

Weigel, D., Beguemsi, T., Garnier, P., Berar, J.F., 1978. Evolution of thermal-expansion tensor as function of temperature .1. General law of evolution of tensor symmetry. J. Solid State Chem. 23, 241-251.

Würflinger, A., 1975. Differential thermal-analysis under high-pressure IV. Low-temperature DTA of solid-solid and solid-liquid transitions of several hydrocarbons up to 3 kbar. Ber. Bunsen-Ges. Phys. Chem. 79, 1195-1201.

Figure Captions

Figure 1. Specific volume of tetrazepam as a function of the temperature obtained from X-ray powder diffraction (open circles) and from single crystal X-ray diffraction at 150 K and 293 K (filled circles). Inset: tetrazepam molecular structure $C_{16}H_{17}ClN_2O$, M = 288.77 g mol^{-1}.

Figure 2. Differential scanning calorimetry curves of racemic monoclinic tetrazepam obtained at 10 K min^{-1}. Curve **(1)** first heating from room temperature of the crystalline monoclinic tetrazepam and curve **(2)** second heating after quenching the melt at 200 K. Inset: enlargement of the glass transition event.

Figure 3. (a) Pressure-temperature phase diagram for the solid-liquid equilibrium and **(b)** melting peaks of tetrazepam at various pressures. Solid and dashed lines in **(a)** correspond to the linear fit (eq. 3) and a power law fit to demonstrate the level of curvature, respectively.

Figure 4. Left panel: Monoclinic structure of tetrazepam at 150 K (*ab* plane). C-H···O and C-H···N intermolecular hydrogen bonds are shown by dashed red and blue lines, respectively. Intramolecular hydrogen bonds are shown by dashed green lines. Right panel: Hirshfeld surface for tetrazepam with neighboring molecules linked through close contacts.

Figure 5. 2D fingerprint plots of tetrazepam (left), diazepam (center) and nordiazepam (right) for the O···H (top) and N···H (bottom) close contacts at room temperature. The (d_i, d_e) frequency increases from dark to light blue. The O···H short contacts correspond to the N-H···O (for example nordiazepam (2.03 Å), see Table 1).

Figure 6. Comparison of the contributions (in percentage) to the Hirshfeld surface areas of a number of intermolecular contacts: O ··· H, N···H, Cl···H, H···H and other minor contributions (C···O, Cl···O, C···Cl, Cl···N, C···C) for tetrazepam, diazepam, and nordiazepam.

Figure 7. α_i eigenvalues of the thermal-expansion tensor as a function of temperature for tetrazepam (top), diazepam (center), and nordiazepam (bottom). The $\boldsymbol{\alpha_2}$ eigenvector is parallel to the two-fold crystallographic axis ***b***. Right top insets correspond to the representation of the second-rank tensors (full length scale of the $\boldsymbol{\alpha_i}$ eigenvectors corresponds to 10^{-4} K^{-1}). Left top insets provide a schematic of the molecule.

Figure 8. The ratio v_L/v_S at the melting triple point as a function of the volume change at the same temperature. The numbers indicate the compound in Table 2. Grey circles correspond to the metastable polymorphs at normal pressure as indicated in Table 2.

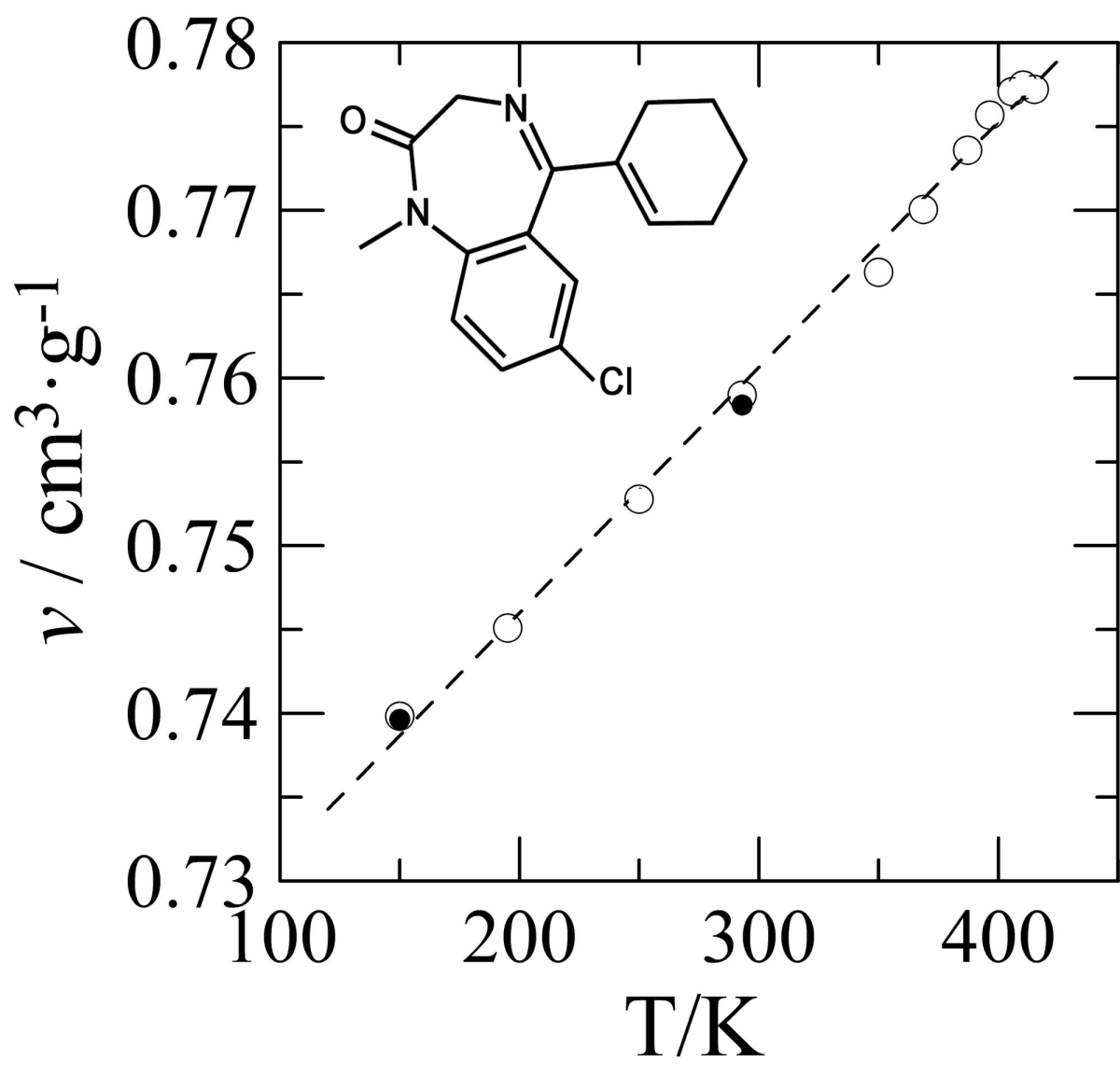
0.78
0.77
0.76
0.75
0.74
0.73
100
200
300
400
T/K
v / cm3·g-1
O
N
N
Cl

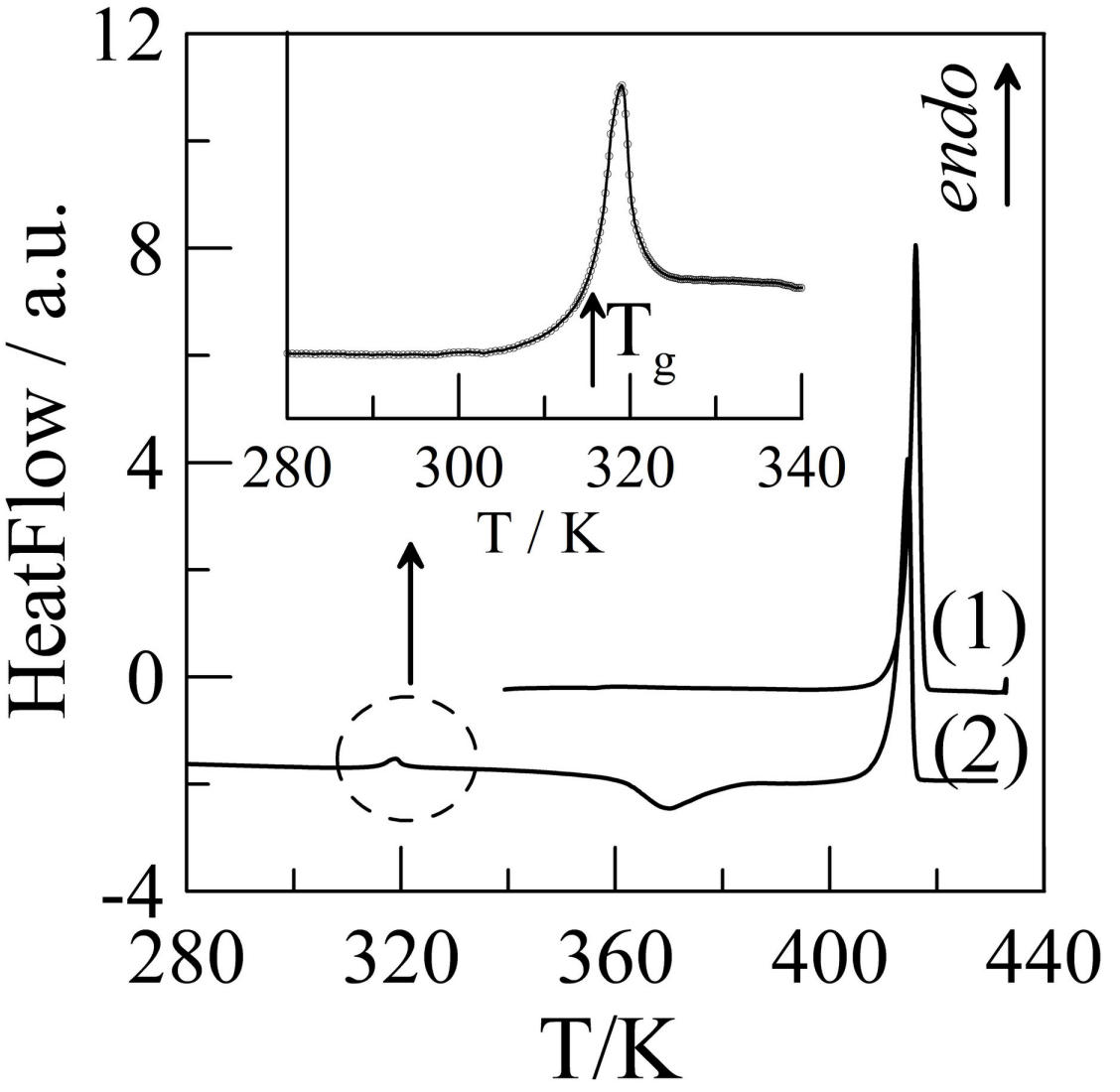
12
8
4
0
-4
HeatFlow / a.u.
endo
280
320
360
400
440
T/K
(1)
(2)
T_g
280
300
320
340
T / K

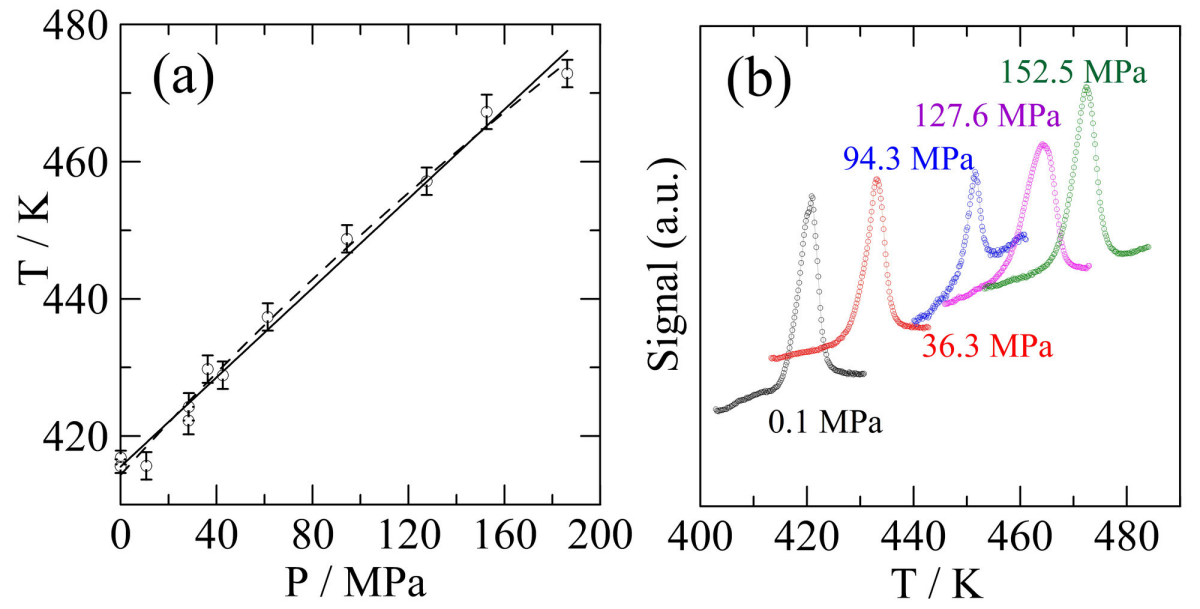
(a)
480
460
440
420
T / K
0
40
80
120
160
200
P / MPa
(b)
152.5 MPa
127.6 MPa
94.3 MPa
36.3 MPa
0.1 MPa
Signal (a.u.)
400
420
440
460
480
T / K

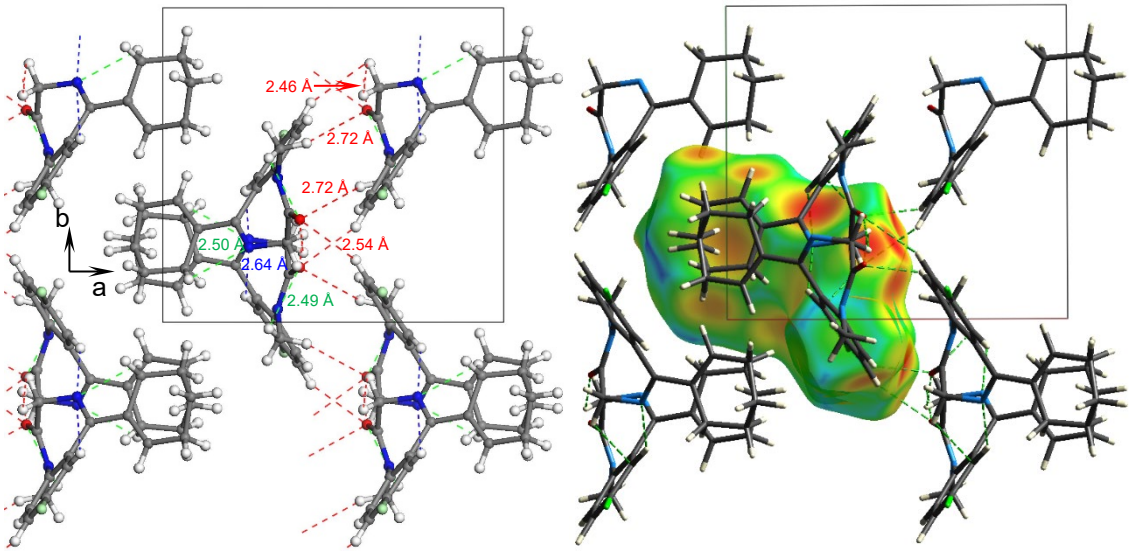
2.46 Å
2.72 Å
2.72 Å
2.50 Å
2.64 Å
2.54 Å
2.49 Å
b
a

Tetrazepam O···H

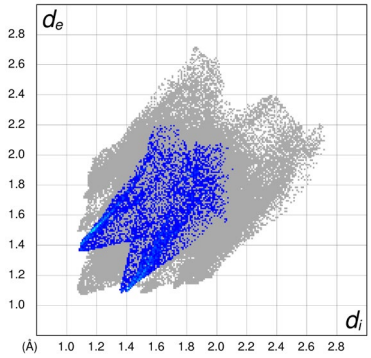

Diazepam O···H

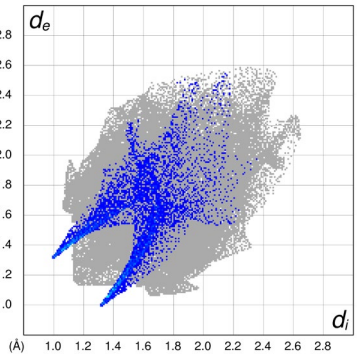

Nordiazepam O···H

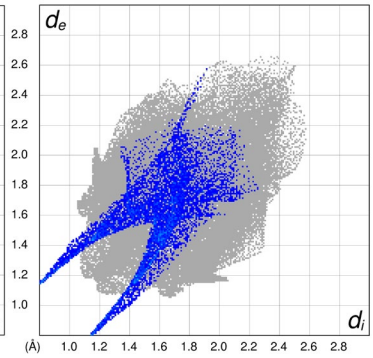

Tetrazepam N···H

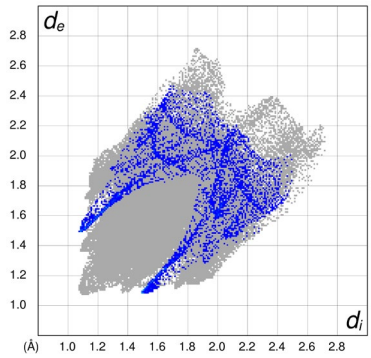

Diazepam N···H

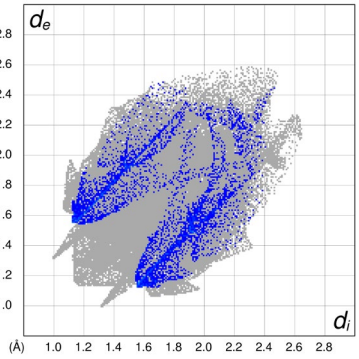

Nordiazepam N···H

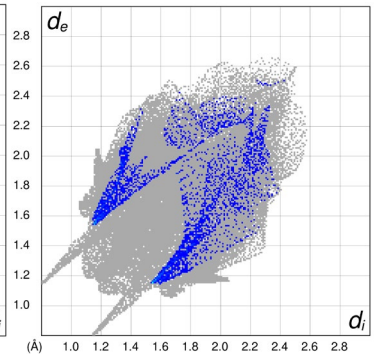

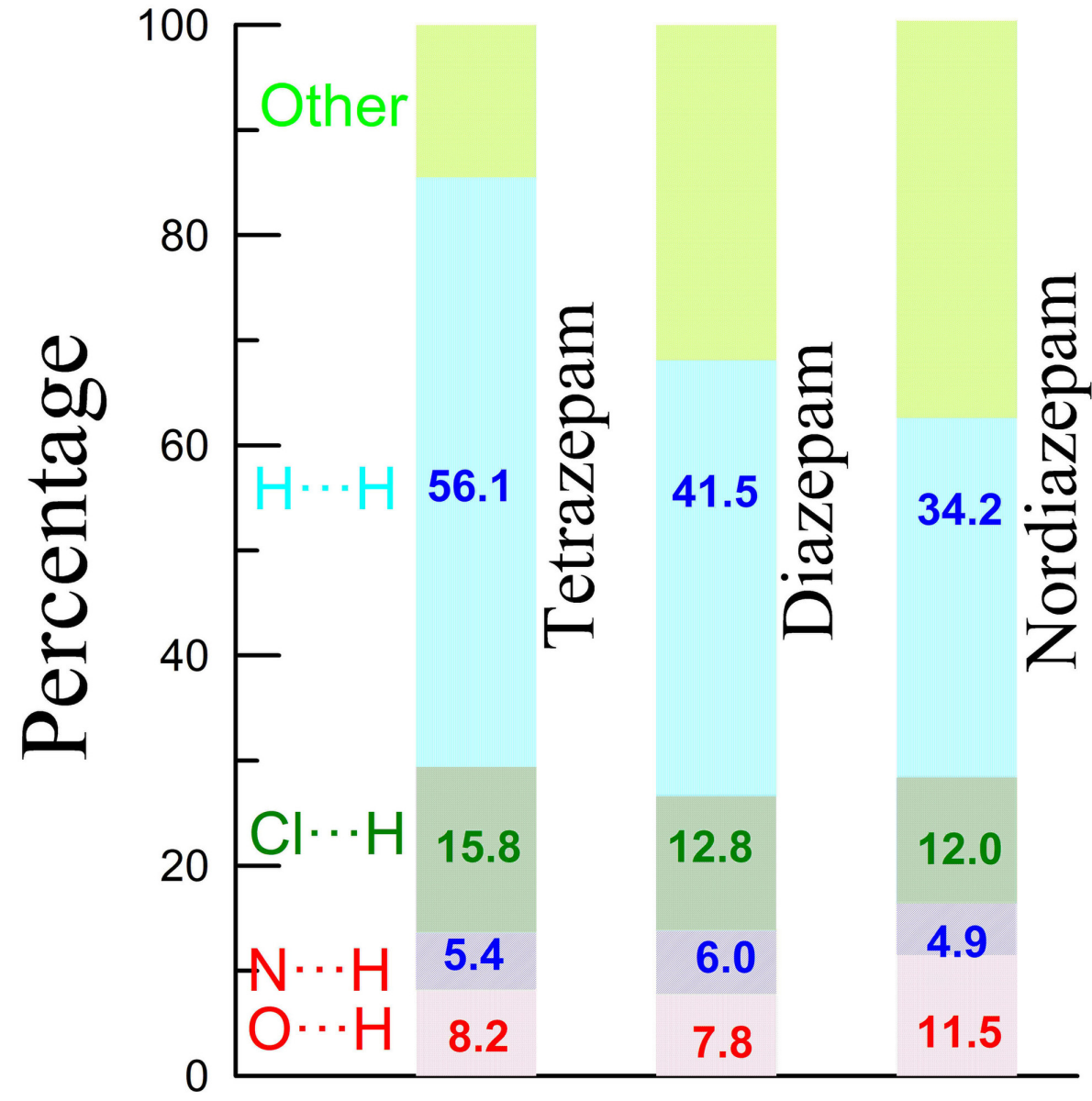
Percentage
100
80
60
40
20
0
Other
H···H
Cl···H
N···H
O···H
56.1
15.8
5.4
8.2
41.5
12.8
6.0
7.8
34.2
12.0
4.9
11.5
Tetrazepam
Diazepam
Nordiazepam

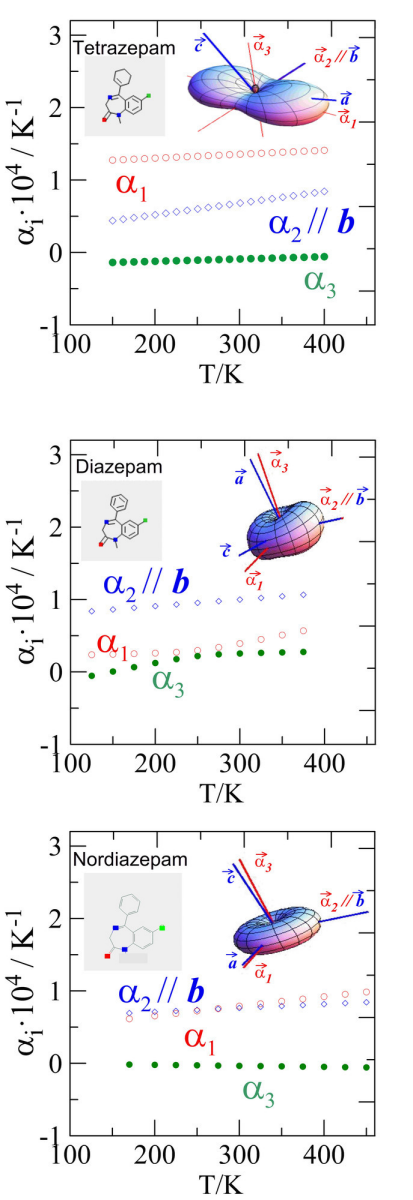
Tetrazepam
$\vec{c}$
$\vec{\alpha}_3$
$\vec{\alpha}_2 // \vec{b}$
$\vec{a}$
$\vec{\alpha}_1$
α_1
$\alpha_2 // \boldsymbol{b}$
α_3
$\alpha_i \cdot 10^4$ / K^{-1}
T/K
Diazepam
$\vec{a}$
$\vec{\alpha}_3$
$\vec{\alpha}_2 // \vec{b}$
$\vec{c}$
$\vec{\alpha}_1$
$\alpha_2 // \boldsymbol{b}$
α_1
α_3
$\alpha_i \cdot 10^4$ / K^{-1}
T/K
Nordiazepam
$\vec{\alpha}_3$
$\vec{c}$
$\vec{\alpha}_2 // \vec{b}$
$\vec{a}$
$\vec{\alpha}_1$
$\alpha_2 // \boldsymbol{b}$
α_1
α_3
$\alpha_i \cdot 10^4$ / K^{-1}
T/K

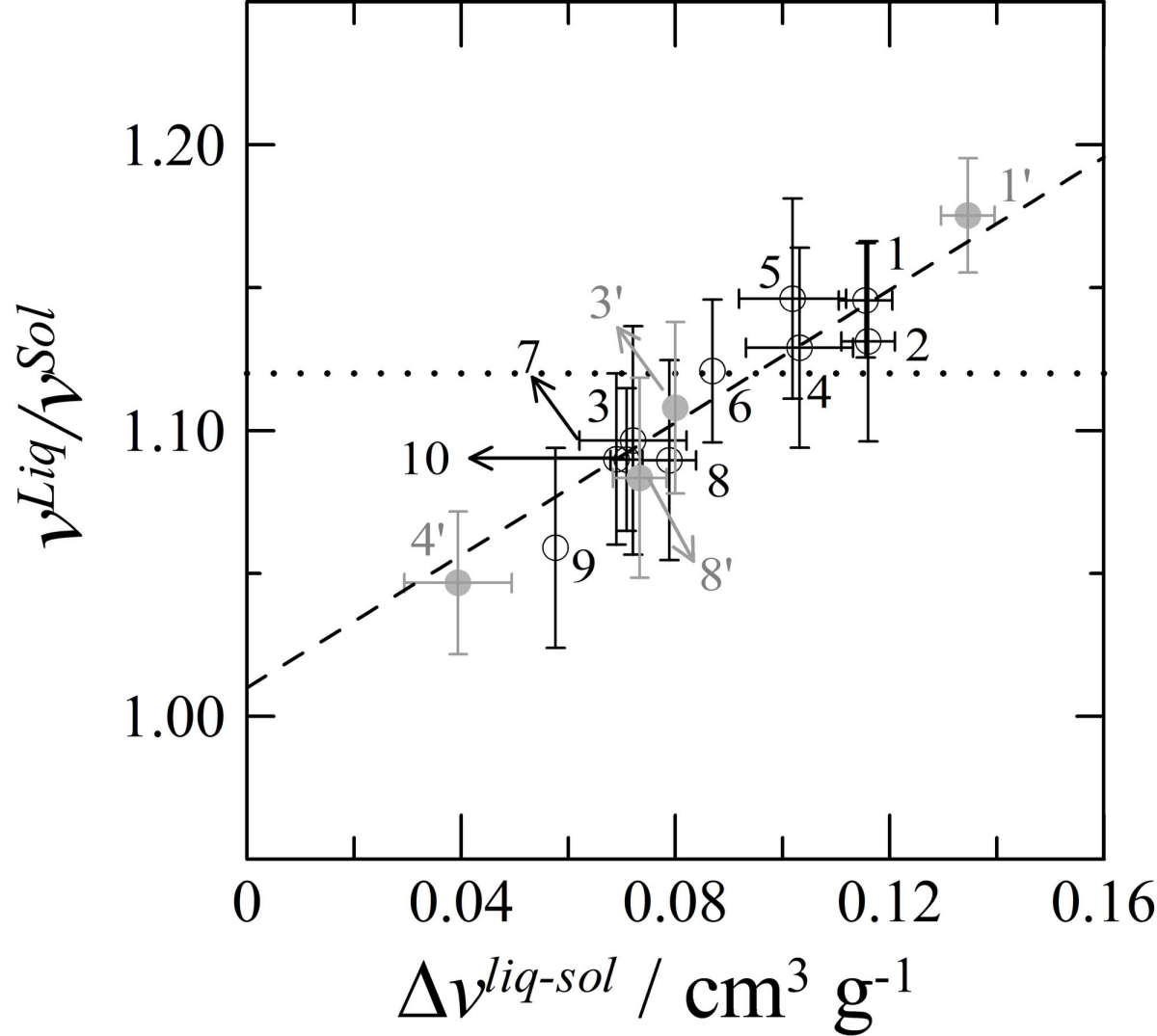
1.20
1.10
1.00
0
0.04
0.08
0.12
0.16
v^{Liq}/v^{Sol}
$\Delta v^{liq\text{-}sol}$ / cm^3 g^{-1}
1
2
3
4
5
6
7
8
9
10
1'
3'
4'
8'

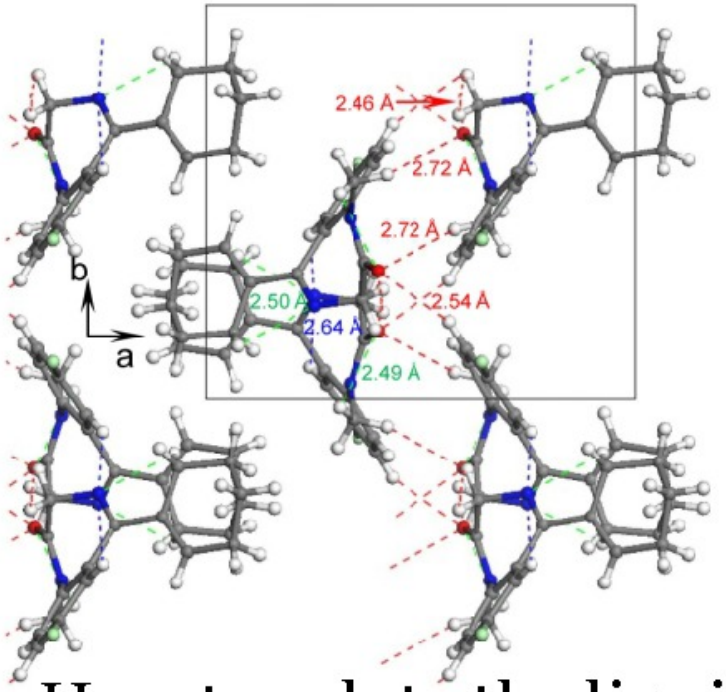

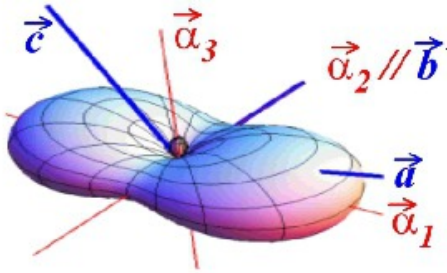

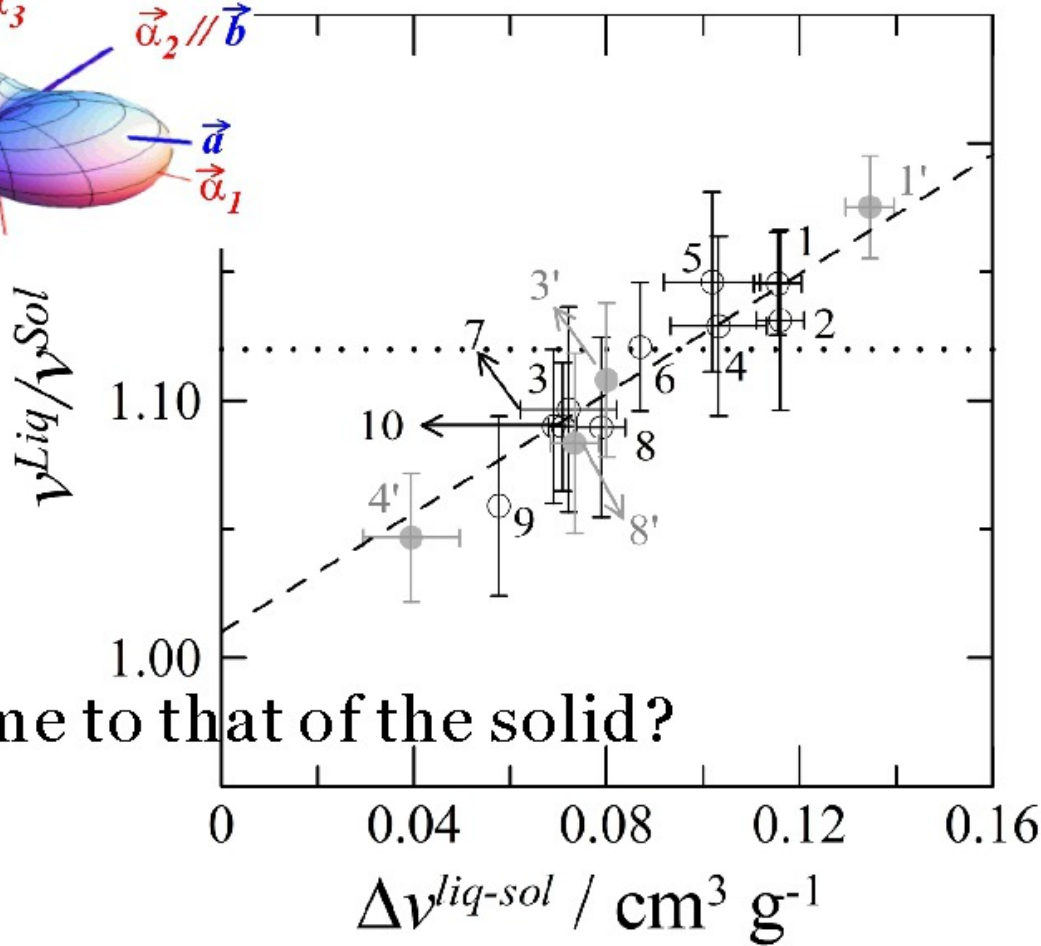

How to relate the liquid volume to that of the solid?